Features of molten pool free surface in laser processing*

YANG Lixin (杨立新) and PENG Xiaofeng (彭晓峰)**

Department of Thermal Engineering, Tsinghua University, Beijing 100084, China

Received February 7, 2001; revised April 11, 2001

Abstract On the basis of static characteristics of free surface of molten pools in laser processing, starting with the change of surface tension, the uniform numerical models are developed for both the liquid and solid regions of metals by applying the enthalpy source method and the porous region model. The flow and heat transfer characteristics in the molten pools and the distribution of surface tension on free surface are disclosed. The shape of free surface is analyzed by considering the static forces on the free surface and by combining with the calculated results of the molten pool. The model is applied to analyzing the laser processing of AISI 304 stainless steel, and the effects of different processing technics and material properties on shaping of free surface are discussed.

Keywords: **molten pool, shape of free surface, surface tension, numerical analysis.**

In high-energy beam processing of metals, the condensing form of free surface will ultimately affect the surface quality of metals. Acted by high-energy laser beam or electronic rays, the metal surface would take the shape of a volcano at the initial instant. As the high-energy beam stops acting, the geometric feature of the volcano crater shape will be kept by sudden cooling of the base material. The shaping of volcano is due to the gradient of surface tension, which makes substances in the center of surface flow toward the brink, and causes the sudden cooling of base material. The condensation features are mainly determined by flow in the molten pool and also concerned with material properties, surface tension, drenching characteristics and parameters used in laser processing. Static force equilibrium of surface tension, applied forces and gravity decide the ultimate shape of molten pool surface.

Very few documents have given a combined analysis on the flow in the molten pool and the shaping of free surface. Refs. [1,2] did not fully take into account the flow and heat transfer in the molten pool and the drenching characteristics.

Applying the enthalpy source method and the porous region model, the present paper develops a uniform numerical method for both the liquid and solid regions of metals, trying to disclose the effects of flow and heat transfer characteristics on free surface. The results are used in calculating the shape of free surface. A model of force equilibrium on free surface is set up and the effects of drenching characteristics and applied force by high-energy laser on surface shaping are analyzed.

* Project supported by the National Natural Science Foundation of China (Grant No. 59625612) and Graduate School of Tsinghua University.

** Corresponding author, E-mail: pxf-dte@mail.tsinghua.edu.cn

1 Analysis of flow and heat transfer in a molten pool

1.1 Boundary conditions of free surface

Generally, the surface tension of free surface (interface of liquid metal and air) of molten metals is a function of gradients of melting component and temperature,

$$\frac{\partial \sigma}{\partial x} = -(C_p \ln T/T_0 + S_0 + C_p) \cdot \frac{\partial T}{\partial x}, \tag{1}$$

where σ is surface tension, x the horizontal coordinate, S_0 and σ_0 are the surface entropy and surface tension respectively at melting point ($T_0 = T_m$), C_p is the heat capacity and T the surface temperature.

Equation (1) shows that the maximum surface temperature T of the molten pool and temperature gradient determine the driving force of surface tension.

In the vicinity of laser beam center, the surface temperature reaches the maximum. The farther from the beam center, the lower the surface temperature is. At the border of the molten pool, the surface temperature is the lowest, which is just the melting point. According to the above equation, the distribution of surface tension is shown in Figure 1.

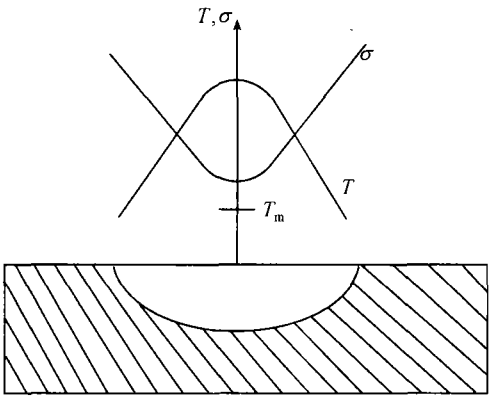

Fig. 1 Distribution of surface temperature and surface tension of molten pool.

AISI 304 stainless steel was analyzed. The relation between surface tension and temperature is expressed as[3]

$$\sigma(T) = \sigma_m - A_\sigma(T - T_m) - R_g T \Gamma_s \ln(1 + Ka_i), \tag{2}$$

where

$$K = k_1 + \exp\left(-\frac{\Delta H_0}{R_g T}\right). \tag{3}$$

Differentiating Eq (2), we have the relation between surface tension and temperature of alloys containing active elements

$$\frac{d\sigma}{dT} = -A_\sigma - R_g \Gamma_s \ln(1 + Ka_i) - \frac{Ka_i}{(1 + Ka_i)} \frac{\Gamma_s H_0}{T}. \tag{4}$$

In calculating the flow and heat transfer in molten pool, we assume that the free surface is in a horizontal plane. The change of gradient of surface tension and surface velocity are coupled into an implicit boundary condition,

$$-\mu \frac{\partial V_r}{\partial n} = \frac{d\sigma}{dT} \frac{\partial T}{\partial r}. \tag{5}$$

1.2 Numerical model inside molten pool

Convective driving forces of melting liquid in the molten pool come from two sources. One is the Marangoni flow by gradient of surface tension, and the other is the buoyancy flow by gradient of horizontal temperature. Melting process is actually a phase-change problem with moving boundary.

Using a liquid fraction scalar, and introducing the enthalpy source into the energy conservation equation and the Darcy source into the momentum conservation equation, we set up the continuity, momentum conservation and energy conservation equations, which make it possible to solve solid region, liquid region and mushy region by fixed grids. For more details about the related model and numerical methods, see References [4 ~ 7].

Numerical simulation of axis-symmetric 2-D flow and heat transfer in the molten pool was made on a sample in laser processing (fig. 2). The distribution of energy of laser beam was parabolic and continuous. The diameter of the laser beam on acting surface was 4mm. The sample was AISI 304 stainless steel with sulfur mass fraction 1×10^{-5}. The material properties are given in Reference [2].

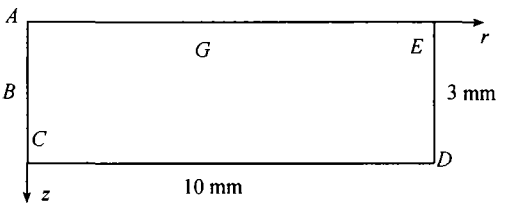

Fig. 2 Geometric model inside the molten pool.

The governing equations of the model are

$$\frac{\partial \rho}{\partial t} + \nabla \cdot (\rho \boldsymbol{U}) = 0, \tag{6}$$

$$\frac{\partial}{\partial t}\rho H + \nabla \cdot \rho \boldsymbol{U} H = \nabla \cdot \lambda \nabla T - \rho_L \left(\frac{\partial f_L}{\partial t}\right), \tag{7}$$

$$\frac{\partial \rho \boldsymbol{U}}{\partial t} + \nabla \cdot (\rho \boldsymbol{U} \otimes \boldsymbol{U}) = -\nabla \cdot P + \nabla \cdot (\mu_L \nabla \boldsymbol{U}) - \frac{\mu_L}{K} U. \tag{8}$$

The boundary conditions of heat transfer at CD, DE and EG regions are

$$h_c(T - T_\infty) = -\lambda \frac{\partial T}{\partial z}, \tag{9}$$

where heat coefficient h_c is a combined heat coefficient of radiation and convective heat transfer, derived from the equation given by Goldak et al.[8],

$$h_c = 24.1 \times 10^{-4} \varepsilon T^{1.61}, \tag{10}$$

where ε is the surface emissivity. Usually ε is 0.9.

1.3 Calculated results of flow and heat transfer inside molten pool

Figure 3 shows the velocity vector distribution inside the molten pool acted by laser beam for 0.3 s. The gradient of surface tension and heat buoyancy force make the molten metal flow from the heating center toward the border, forming two vortices (Figure 4).

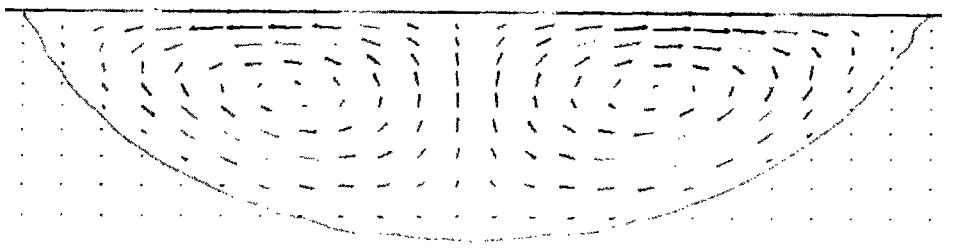

Fig. 3 Velocity distribution inside the molten pool.

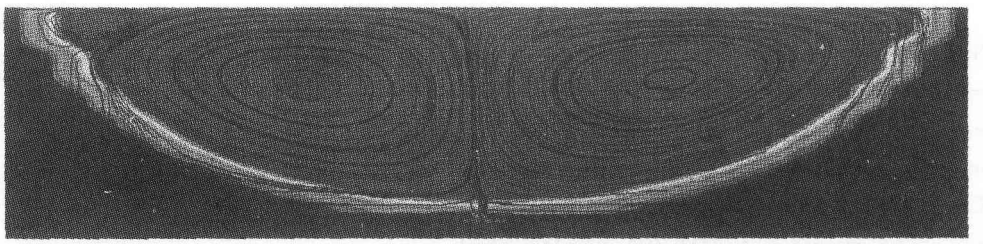

Fig. 4 Streamlines inside the molten pool.

The distributions of velocity, temperature and surface tension on free surface of the molten pool are the basic data for further analysis of surface shape. Fig. 5 gives the velocity distribution of free surface. The minimum velocity is located in the middle of heating center and the border.

The temperature distribution on free surface is shown in Fig. 6. Eq. (2) gives the distribution of surface tension coefficient on free surface. The calculated results show good consistency with the analysis in the previous section. The shape of free surface can be obtained from the distribution of surface tension coefficient and force equilibrium on free surface.

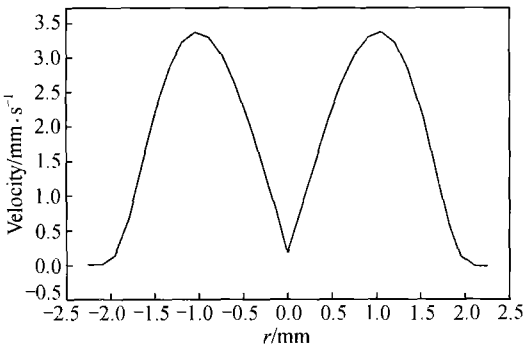

Fig. 5 Velocity distribution on the molten pool surface.

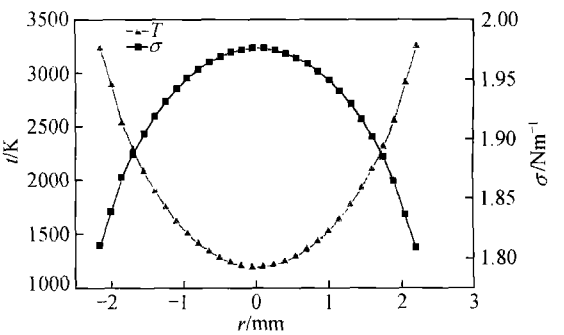

Fig. 6 Distributions of surface temperature and surface tension.

2 Free surface of molten pool

Assuming that the free surface shape is as shown in Fig. 7, the local coordinate could be set up. For gas-liquid interfacial surface we have the Young-Laplace equation.

$$P_{\mathrm{I}} - P_{\mathrm{II}} = \sigma\left(\frac{1}{r_1} + \frac{1}{r_2}\right), \tag{11}$$

where P_{I} is the pressure of concave side, P_{II} the pressure of convex side, σ the surface tension of gas-liquid interfacial surface, and r_1, r_2 are two main curvature radii.

$$P_{\mathrm{I}} = P_{\mathrm{I0}}(x) + \rho_{\mathrm{I}} gz, \tag{12}$$

$$P_{\mathrm{II}} = P_{\mathrm{II0}} + \rho_{\mathrm{II}} gz. \tag{13}$$

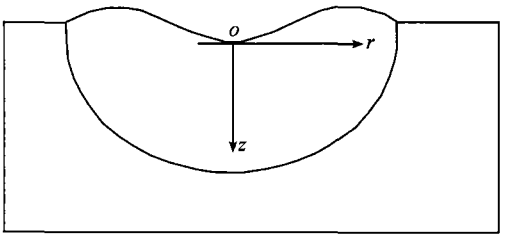

Fig. 7 Analytical coordinate of the free surface.

Assuming that the applied pressure field is parabolic, we have

$$P_{\mathrm{I}} = -Ax^2 + C + \rho_{\mathrm{I}} gz = P_{\mathrm{I0}} + \rho_{\mathrm{I}} gz - Ax^2, \tag{14}$$

where $P_0(x)$ is the distribution of the applied pressure field, and $P_{\mathrm{I0}} = C_0$, P_{I0} and P_{II0} are pressures of the two phases at $(0,0)$. According to the Young-Laplace equation,

$$P_{\mathrm{I0}} - P_{\mathrm{II0}} = \frac{2\sigma}{r_0}. \tag{15}$$

The geometrical relationship gives the following equations:

Curvature radius normal to surface,

$$\frac{1}{r_1} = \frac{\dfrac{\mathrm{d}^2 z}{\mathrm{d}r^2}}{\left[1 + \left(\dfrac{\mathrm{d}z}{\mathrm{d}r}\right)^2\right]^{3/2}}; \tag{16}$$

Curvature radius in drawing plane,

$$\frac{1}{r_2} = \frac{\dfrac{\mathrm{d}z}{\mathrm{d}r}}{r\left[1 + \left(\dfrac{\mathrm{d}z}{\mathrm{d}r}\right)^2\right]^{1/2}}. \tag{17}$$

Introducing dimensionless parameters ξ and λ, $\xi = \dfrac{z}{r_0}$, $\lambda = \dfrac{r}{r_0}$, we obtain the dimensionless shape equation

$$\frac{\xi''}{[1 + (\xi')^2]^{3/2}} + \frac{\xi'}{\lambda[1 + (\xi')^2]^{1/2}} = 2 - B_0\xi - A_0\lambda^2, \tag{18}$$

where $B_0 = \dfrac{(\rho_1 - \rho_{\mathrm{v}})gr_0^2}{\sigma}$, $A_0 = \dfrac{Ar_0^3}{\sigma}$, and r_0 is the radius of curvature at $(0,0)$.

The fourth order Longue-Kuta method was adopted to simulate Eq. (18). The pressure of liquid phase side was unknown at the initial iteration, i.e. the value of r_0 was not certain. So an initial value of r_0 was assumed according to the applied pressure. It was 0.012 mm when the applied pressure was 300 Pa at $(0,0)$. In practical physical process, as the pressure on gas side increases, the center of free surface moves down, the pressure on liquid phase side increases, and then r_0 increases. If the

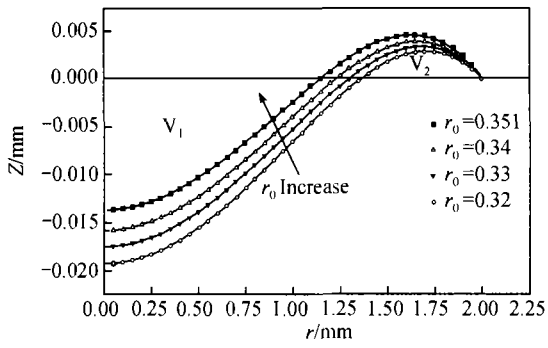

Fig. 8 Effects of r_0 on free surface shape.

evaporation of mass is neglected, the final shape of free surface should ensure that equal volumes of V_1 and V_2 satisfy the mass conservation of liquid phase (Fig. 8). Through iteration by increasing the value of r_0 until the mass conservation is satisfied, the final curve of free surface can be obtained.

Figure 8 shows the shape variation of free surface at different r_0 values. The width of molten pool was obtained from the results of numerical simulation inside the molten pool. In the calculation the half-width of pool was 2 mm. The curve of $r_0 = 0.3516$ represents the free surface shape of the sample in this case.

The calculations of free surface shapes are discussed below.

2.1 Effects of applied pressure field on shape of molten free surface

In laser processing, the applied pressure is an integrated pressure of laser beam or electronic ray and protecting inert gas. Its value can be measured. It is assumed to be a parabolic distribution in this study. Fig. 9 shows the curves of free surface change at different maximum center pressures of 300, 350 and 400 Pa. According to fig. 9, as pressure increases, the center of free surface moves down and the distance between wave crest and trough increases. The rate of slope increases at the solid-liquid interfacial point; that is, the contact angle rises.

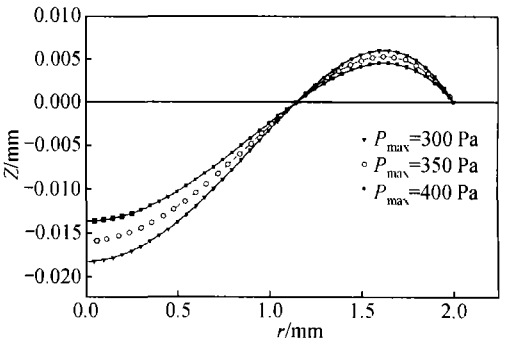

Fig. 9 Effects of applied pressure field on free surface shape.

The boundary shape is determined by equilibrium of surface tensions at gas-liquid, gas-solid and solid-liquid interfacial surfaces. The Young equation gives

$$\sigma_{lv}\cos\theta_e = \sigma_{sv} - \sigma_{sl}, \tag{19}$$

where σ_{lv}, σ_{sv} and σ_{sl} are surface tensions at gas-liquid, gas-solid and solid-liquid interfacial surfaces respectively; θ_e is the balanced contact angle of three phases. However, in practical physical process, because of the existence of surface roughness, the contact angle observed is not unique as the Young Equation describes, but varies within a certain range. The maximum value of contact angle is called the advancing contact angle, while the minimum is called the receding contact angle. If the varying liquid status is considered to change the solid-liquid and gas-liquid interfacial tensions, the variations of contact angles do not contradict the Young equation. A more acceptable explanation is the Wenzel contact angle proposed by Wenzel in 1936. He deemed that the Young equation did not generally describe the balanced solid-liquid action. If solid surfaces are rough, for the solid-liquid and gas-solid surface tensions, one should refer to the real surface area instead of the geometric sur-

face area. Let γ = geometric surface area/Peal surface area. Then the Wenzel Equation gives

$$\sigma_{lv}\cos\theta_w = \gamma(\sigma_{sv} - \sigma_{sl}), \quad (20)$$

where θ_W is the Wenzel contact angle. The surface shape at the solid-liquid boundary is constrained by the Wenzel contact angle and varies with different solid surface properties, which is a limiting boundary condition, meaning that as the applied pressure increases and the boundary contact angle is larger than the Wenzel contact angle, the balance at that point cannot be kept. The free surface collapses and the molten liquid drains out of the border and the model is no longer valid.

2.2 Effects of distribution of surface tension on shape of molten pool

According to the analysis of free surface tension of the molten pool, the surface tension coefficient changes with temperatures. The above results of flow and heat transfer give the distribution of surface tension coefficient (Fig. 6). Fig. 10 shows the calculated free surface shapes of the molten pool with constant (the value at the center point) or varying surface tension coefficient. It also shows that the change of gradient of surface tension makes molten surface contract.

2.3 Comparison of molten pool depth and fluctuation magnitude of free surface

According to the above analysis, when the depth of molten pool is 1 mm and half-width is 2 mm, the fluctuation magnitude of free surface is about 0.02 mm, which is much smaller than the depth or width value. The analysis of heat transfer indicates that the temperature difference in the depth of 0.02 mm is about 300 K, which induces a variation of surface tension coefficient of about 0.03. So the effects of free surface fluctuation can be neglected in the calculation of flow and heat transfer of the molten pool. The assumption in Section 1, which considers the free surface as a plane, is reasonable. This assumption simplifies the simulation model and related calculation tasks.

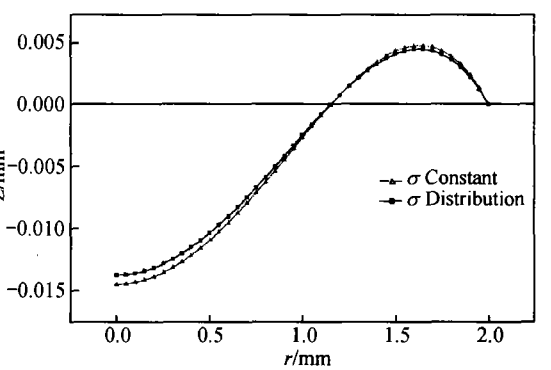

Fig. 10 Free surface shape under different surface tensions.

3 Conclusions

A complete simulation model for analyzing molten pool surface in laser processing has been established. From analyses of a practical molten test sample of AISI 304 stainless steel, the following conclusions can be drawn.

(i) The model can be used to simulate free surface shape in most high-energy beam processing (pulse laser and electronic ray).

(ii) The free surface of molten pool is affected by material properties, surface tension, drenching characteristics and processing techniques, and also related to flow characteristics inside the molten pool. The effects of applied pressure and surface tension are more notable.

(iii) The Marangoni flow caused by the gradient of surface tension determines the internal flow

and free surface shape.

(iv) Because of the limitation of advancing contact angle, as the applied pressure is increasing, the free surface of molten pool would collapse at the border.

In consideration of evaporation during laser processing, further research on free surface of molten pool shoul be made with an amended changing volume model based on the present work.

Nomenclature

a_i, Mass fraction of active substance;
A_γ, Constant of surface tension gradient, $N \cdot m^{-1} \cdot K^{-1}$;
C_P, Heat Capacity at constant pressures, $J \cdot kg^{-1} K^{-1}$;
f_L, Liquid fraction;
h_c, Combined heat transfer coefficient, $W \cdot m^{-2} \cdot K^{-1}$;
ΔH_0, Standard absorbing heat, $J \cdot kg^{-1} \cdot mole^{-1}$;
R_g, Gas constant, $J \cdot kg^{-1} \cdot mole^{-1} \cdot K^{-1}$;
r_0, Radius of curvature at center, m;
T, Temperature, K;
U, Mixing velocity, $m \cdot s^{-1}$;
Γ_s, Surface saturation redundancy, $J \cdot kg^{-1} \cdot mole^{-1} \cdot m^{-2}$;
β, Coefficient of heat expansion, K^{-1};
ε, Surface emissivity;
λ, Thermal conductivity, $W \cdot m^{-1} \cdot K^{-1}$;
μ, Dynamic viscosity, $kg \cdot m^{-1} \cdot s^{-1}$;
ρ, Density, $kg\ m^{-3}$;
σ, Surface tension, $N \cdot m^{-1}$;
σ_m, Surface tension at melting point, $N \cdot m^{-1}$;
$d\sigma/dT$, Gradient of surface tension, $N \cdot m^{-1} \cdot K^{-1}$.

References

1 Thompson, M. E. et al. The transient behavior of weld pools with a deformed free surface. Int. J. Heat Mass Transfer, 1989, 32(6): 1007.
2 Choo, R. T. C. et al. Modeling of high-current arcs with emphasis on free surface phenomena in the weld pool. Weld. J., Res. Suppl., 1990: 346.
3 Sahoo P, et al. Surface tension of binary metal surface active solute systems under conditions relevant to welding metallurgy. Metall. Trans. B 1998, 19B: 483.
4 Voller, V. R. et al. General source-based method for solidification phase change. Numerical Heat Transfer, Part B, 1991, 19: 175.
5 Bennon, W. D. et al. A continuum model for momentum, heat and species transport in binary solid-liquid phase change systems-I. Model formulation, Int. J. Heat Mass Transfer, 1987, 30: 2161.
6 Yang, L. X. et al. Numerical model of melting and solidification in laser process (in Chinese), In: Collection of Heat and Mass Transfer Conference, Jinan, 2000, 280.
7 Reza, M. et al. Coupled turbulent flow, heat and solute transport in continuous casting processes. Met. Trans. B. 1995, 26B: 731.
8 Goldak, J, et al. Computer modeling of heat flow in welds. Metall. Trans., 1986, 17B: 587.